ACS Macro Letters

Letter

pubs.acs.org/macroletters

Nanoscale Phase Behavior of Mixed Polymer Ligands on a Gold Nanoparticle Surface

Seyong Kim,[†] Tae-Hwan Kim,[‡] June Huh,*[,†] Joona Bang,*[,†] and Soo-Hyung Choi*[,§]

[†]Department of Chemical and Biological Engineering, Korea University, Seoul, 136-701, Republic of Korea

[‡]Neutron Science Division, Korea Atomic Energy Research Institute (KAERI), Daejeon, 305-353, Republic of Korea

[§]Department of Chemical Engineering, Hongik University, Seoul, 121-791, Republic of Korea

Supporting Information

ABSTRACT: The phase behavior of mixed polymer ligands anchored on Au nanoparticle surfaces was investigated using small-angle neutron scattering (SANS). An equimolar mixture of deuterated polystyrene (*d*PS) and normal poly(methyl methacrylate) (PMMA) was attached to Au nanoparticles, and the polymer-grafted nanoparticles were characterized in an isotopic toluene mixture, a good solvent for both homopolymers. Poly(deuterated styrene-*ran*-methyl methacrylate) (P(*d*S-*r*-MMA)) attached to the Au nanoparticles was also characterized as a control case. The results suggest that as the molecular weight increases, the two species of polymers become phase-separated on the nanoparticle surface, resulting in the formation of Janus-type nanoparticles. Monte Carlo simulations for the model polymer-grafted particle system suggest that the effective attraction between the polymers and the particle leads to dense wetting layers of solvophilic polymer blends in the vicinity of the solvophobic particle surface, which plays a decisive role in the formation of the phase-separated morphology.

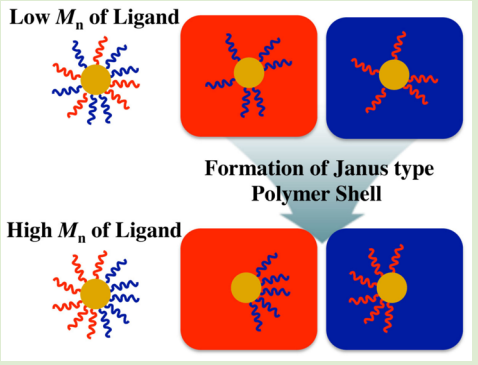

The incorporation of inorganic nanoparticles into a polymeric matrix has been widely employed to improve the mechanical, electrical, and optical properties for the complex materials.[1−4] In general, the high incompatibility between the nanoparticles and polymers results in a phase separation, which prevents the achievement of the desired performance of these systems. Surface modification by attaching polymers or oligomers on the nanoparticles, however, improves the compatibility and stability, resulting in well-dispersed nanoparticles in the polymeric matrix.[5−7] Furthermore, the location of the nanoparticles in the block copolymer system and the surface activeness can be delicately tuned by the coverage or moiety of polymer ligands attached to the surface.[8−15] Recently, two types of polymers were attached to nanoparticles to alleviate the interfacial tension in the block copolymer system.[16,17] These works clearly demonstrate that the nanoparticles covered by two species of polymer ligands show an amphiphilic property, which may suggest the phase separation of the two polymer ligands on the nanoparticle surface.[18−20] However, it was unclear whether the phase separation is induced by the interaction between the polymer ligands or by the surrounding medium, analogous to an induced dipole under an external electric field. Nonetheless, very few works have yet evaluated the phase behavior of mixed polymer ligands attached to nanoscale surfaces (~100 nm^2) due to the limitations of either/both characterization technique and experimental materials.[19−21]

It is possible to characterize the structure of polymer or oligomer blends attached to nanoparticles using transmission microscopy (TEM), scanning tunneling microscopy (STM), fluorescence, and spectroscopic techniques.[22−25] Because most techniques require elaborate data analysis or postmodification, such as staining, they are limited to the investigation of the phase behavior of ligand blends on a nanoscale surface.[26,27] Recently, Stellacci et al. presented a simple but comprehensive method to investigate the phase behavior of two types of oligomers (e.g., aliphatic and aromatic ligands) on Au nanoparticles using two-dimensional (2D) NMR.[25] Unfortunately, the spectroscopy technique requires a short distance (<0.5 nm) between ligands, which cannot be satisfied by a polymeric ligand system.[28] To the best of our knowledge, small-angle neutron scattering (SANS) is the best tool to characterize the phase behavior of mixed polymer ligands anchored to nanoparticle surfaces. The scattering factor for Janus particles developed by Fütterer et al. provides a positive methodology to distinguish Janus-shell particles from mixed-shell particles using SANS.[29]

In this study, we have investigated the phase behavior of deuterated polystyrene (*d*PS) and poly(methyl methacrylate) (PMMA) homopolymer ligands attached to Au nanoparticles dispersed in toluene, neutrally good for both polymer ligands, using SANS. Thiol end-functionalized *d*PS and PMMA homopolymers and random copolymers of *d*PS and PMMA (1:1 molar feed ratio), as a counterpart, were synthesized using

Received: February 9, 2015
Accepted: March 27, 2015
Published: March 30, 2015

DOI: 10.1021/acsmacrolett.5b00101
ACS Macro Lett. 2015, 4, 417−421

reversible addition−fragmentation chain transfer (RAFT) polymerization (Supporting Information, Scheme S1). Each includes three different molecular weights with a narrow distribution: ∼3000, ∼7000, ∼15000 g/mol. The molecular characteristics of the polymer ligands are listed in Table 1.

Table 1. Characteristics of Polymer Ligands and Au Nanoparticles

Au NPs type	ligand	M_n (g/mol)	dispersity ($Đ$)	R_{core} (nm)	R_{ptcl} (nm)
Mixed-1	*d*PS-1	3200	1.12	1.36	3.90
	PMMA-1	3300	1.23		
Mixed-2	*d*PS-2	6900	1.08	1.38	5.95
	PMMA-2	7200	1.30		
Mixed-3	*d*PS-3	17700	1.09	1.43	8.15
	PMMA-3	15300	1.25		
Random-1	P(*d*S-*r*-MMA)-1	2900	1.18	1.46	3.43
Random-2	P(*d*S-*r*-MMA)-2	6800	1.17	1.44	6.10
Random-3	P(*d*S-*r*-MMA)-3	15400	1.14	1.48	7.90

Polymer-grafted Au particles were prepared by the two-phase method using an equimolar mixture of *d*PS and PMMA ligands, referred to as "Mixed", and random copolymer ligands, referred to as "Random". For example, Mixed-1 and Random-1 indicate Au nanoparticles grafted with an equimolar mixture of end-grafted *d*PS-1 and PMMA-1, and P(*d*S-*r*-MMA)-1, respectively. The detailed experimental method is described elsewhere.[15,16] Table 1 also lists the average radius of the Au core (R_{core}) and the hydrodynamic radius of polymer-grafted nanoparticles (R_{ptcl}) in toluene, measured by transmission electron microscope (TEM) and dynamic light scattering (DLS), respectively (see Supporting Information). The grafting densities estimated from TGA weight loss were 1.52, 1.40, and 1.24 chains/nm^2 for Mixed-1, Mixed-2, and Mixed-3, respectively, given that the mean diameter of Au particle is ∼3 nm. A rough estimation of molecular weight dependence on the height of grafted chain using the theoretical scaling suggests that the grafted polymers at these grafting densities are in the regime of semidilute brush rather than in the regime of concentrated brush based on the theoretical scaling form for spherically grafted polymers (see Figures S1 and S2 and also a note in ref 32).[30−32]

SANS experiments were performed with the 40 m SANS instrument at HANARO, Korea Atomic Energy Research Institute, with a neutron wavelength of λ = 6 Å ($\Delta\lambda/\lambda$ = 0.12). Specimens were loaded in a quartz banjo cell, and exposed to the beam at room temperature for at least 90 min. SANS specimens were prepared by dispersing 4 wt % of the nanoparticles in a mixture of deuterated and protonated toluene. The scattering length densities (SLD) of the Au, *d*PS, PMMA, protonated toluene, and deuterated toluene are 4.51, 6.46, 1.06, 0.94, and 5.66 × 10^{10} cm^{-2}, respectively. The SLD of the isotopic mixture solvent is estimated as $SLD_{sol} = SLD_{p\text{-toluene}}\phi_{p\text{-toluene}} + SLD_{d\text{-toluene}}(1 - \phi_{p\text{-toluene}})$, where $\phi_{p\text{-toluene}}$ is the volume fraction of protonated toluene in the solvent mixture. Here, SLD_{sol} was selected as 1.06 (matched to PMMA), 2.50, 3.50, 4.51 (matched to Au), and 5.66 (matched to pure deuterated toluene) × 10^{10} cm^{-2} for the contrast variation experiment.

Figure 1 displays the SANS patterns obtained from (a) Mixed-1, (b) Mixed-3, (c) Random-1, and (d) Random-3 specimens in the five isotopic toluene mixtures. The first minimum of the profile, usually corresponding to the core

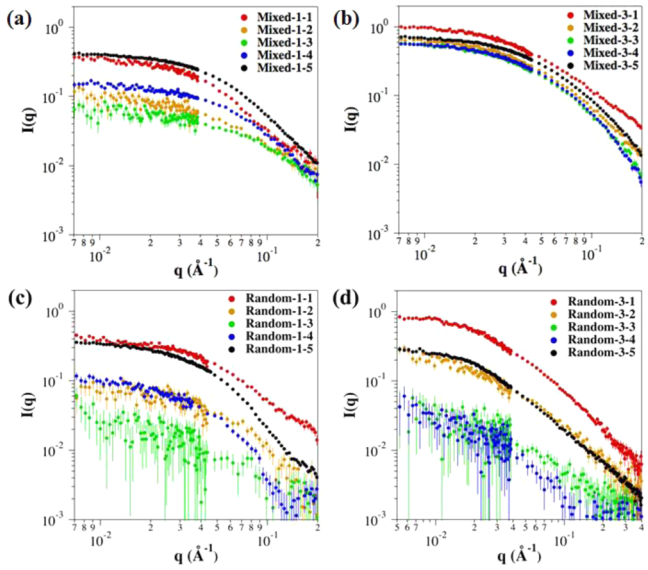

Figure 1. SANS profile obtained from (a) Mixed-1, (b) Mixed-3, (c) Random-1, and (d) Random-3 in the five isotopic mixtures of toluene. SLDs of the solvent mixture (i.e., the second digits in the sample labels from 1 to 5) correspond to 1.06, 2.50, 3.50, 4.51, and 5.66 × 10^{10} cm^{-2}.

radius for the nanoparticle system, cannot be distinguished in the experimental range, which can be attributed to the relatively large dispersity in the Au core radius (Supporting Information, Figure S3). It should be noted that the scattering intensity obtained from the Mixed-3 specimen is nearly insensitive to SLD_{sol}, whereas the other specimens show strong dependences of the scattering intensity on SLD_{sol}. The SANS intensity is proportional to the contrast factor of both the polymer shell and Au core as $(SLD_x - SLD_{sol})^2$, where x denotes either the polymer shell or Au core. As SLD_{sol} increases, the Au core contribution to the SANS intensity varies similarly and consistently for both the Mixed and Random samples and therefore cannot provide the different SLD_{sol} dependence. However, the polymer shell contribution to the SANS intensity depends on the distribution of monomers and thus the shell morphology.

Along with polymer blend melts, it is reasonably assumed that two polymers of equal molecular weight grafted to a nanoparticle surface form mixed or separated phases, the latter of which are known as Janus-type particles. It has been suggested that the SLD_{sol} dependence of SANS intensity at $3 < qR_{ptcl} < 4$ can be regarded as strong evidence to distinguish Janus-shell particles from mixed-shell particles due to the particle symmetry.[29] Figure 2 shows the scattering intensity of $3 < qR_{ptcl} < 4$ obtained from (a) Mixed-1 and Random-1, (b) Mixed-2 and Random-2, and (c) Mixed-3 and Random-3 as a function of SLD_{sol}. For Random specimens, the SLD of the polymer shell can be estimated as 3.76 × 10^{10} cm^{-2}, average values of SLD_{dPS} and SLD_{PMMA}, because the *d*PS and PMMA monomers are randomly distributed in the shell. Considering an SLD_{Au} of 4.51 × 10^{10} cm^{-2}, the scattering intensity obtained from all Random specimens shows a minimum at SLD_{sol} = 3.50 × 10^{10} cm^{-2} (Random-1, Random-2) or at SLD_{sol} = 4.51 × 10^{10} cm^{-2} (Random-3), as expected. In contrast, the SLD_{sol} dependence of the scattering intensity for Mixed specimens significantly depends on the distribution of the two polymers. When *d*PS and PMMA are completely mixed, the SLD of the

DOI: 10.1021/acsmacrolett.5b00101
ACS Macro Lett. 2015, 4, 417−421

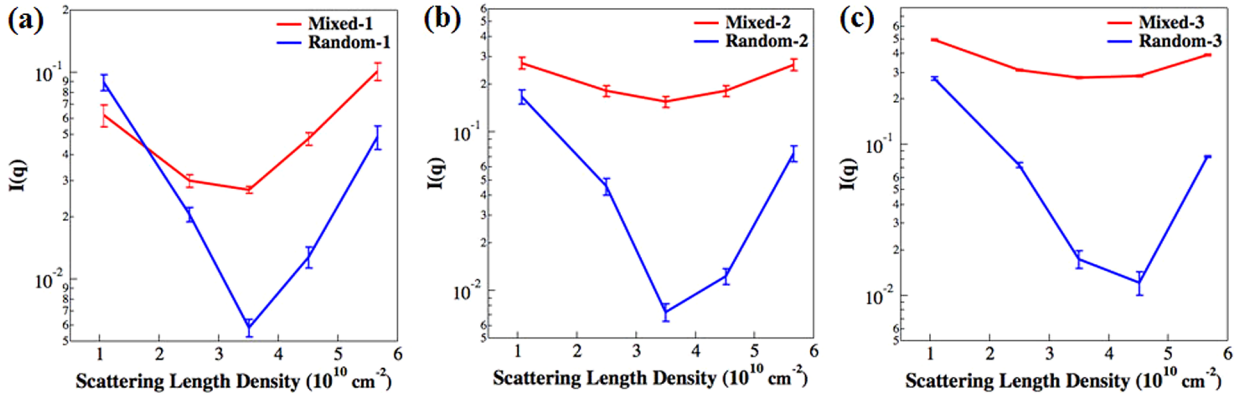

Figure 2. SLD_{sol} dependence of scattering intensity of $3 < qR_{ptcl} < 4$ (where R_{ptcl} is the hydrodynamic radius of the nanoparticles) obtained from (a) Mixed-1 and Random-1, (b) Mixed-2 and Random-2, and (c) Mixed-3 and Random-3. The corresponding q value are 0.0621 Å^{-1} < q < 0.0895 Å^{-1}, 0.0385 Å^{-1} < q < 0.0655 Å^{-1}, and 0.0360 Å^{-1} < q < 0.0388 Å^{-1} for (a), (b), and (c), respectively.

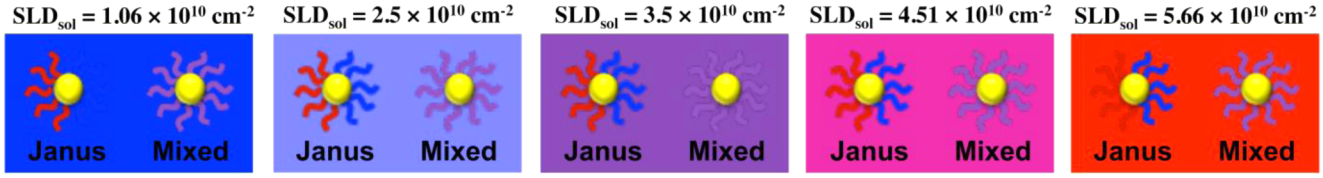

Figure 3. Schematic figure to distinguish Janus-shell particles from mixed-shell particles using contrast variation measurement of SANS. The contrast for mixed-shell particles can be matched to the background, resulting in weak scattering, but the contrast for Janus shell cannot be matched out.

mixed shell is estimated as the same value as that of the Random ligand, 3.76 × 10^{10} cm^{-2}, and therefore the SANS intensity as a function of SLD_{sol} shows the same behavior as for the Random specimens. The scattering intensity obtained from completely demixed *d*PS and PMMA, that is, Janus-shell particles, however, is nearly invariant to SLD_{sol} because SLD_{sol} cannot be completely matched to the polymer shell (Figure 3). The SLD_{sol} dependence of the scattering intensity for Mixed-2 and Mixed-3 is relatively weak, suggesting that the *d*PS and PMMA ligands for Mixed-2 and Mixed-3 are segregated to form phase-separated surface domains. For Mixed-1, the SANS intensity shows a pronounced minimum at SLD_{sol} = 3.50 × 10^{10} cm^{-2} in the contrast variation measurement, as with the case of Random-1. Therefore, it can be deduced that *d*PS and PMMA of low molecular weight are either mixed or partly demixed.

For symmetric binary homopolymer blends (equimolar homopolymer mixture with an equal molecular weight) in the presence of a neutral solvent, demixing occurs above a critical value of $\chi N = 2/\phi$, where χ is the Flory–Huggins interaction parameter between two monomers, N is the degree of polymerization, and ϕ is the volume fraction of polymer in the solution. In our system, the χN values at 20 °C are estimated to be 1.2, 2.8, and 6 for Mixed-1, Mixed-2, and Mixed-3, respectively.[34,35] With the rough assumption that the behavior of the mixed polymer ligands attached to a two-dimensional (2D) surface is similar to that of a concentrated polymer blend solution, the estimated χN values suggest that ϕ must have values greater than 0.72 and 0.33 for Mixed 2 and Mixed 3, respectively, to make the mixed polymer ligands undergo phase separation. This requirement implies that toluene, a good solvent for both polymers, is expelled from the polymer shell. This counterintuitive result can be understood by the pairwise interactions between the components in the nanoparticle solutions. Table 2 lists pairwise values of the interfacial tension for the system components.

Table 2. Pairwise Values of Interfacial Tension for PS, PMMA, Toluene, and Au at Room Temperature

(dyn/cm)	PS	PMMA	toluene	Au
PS[a]		1.1	1.6	3.1
PMMA[a]	1.1		3.6	2.3
toluene[b]	1.6	3.6		8.9
Au[a]	3.1	2.3	8.9	

[a]Estimates from the measurements of the contact angles of water and diiodomethane as reference drops on the surface (PS, PMMA, Au) using the Young–Owens–Wendt equation.[33] [b]Estimate from the measurements of the contact angle of toluene on the reference surface (poly(tetrafluoroethylene)) using the Young–Owens–Wendt equation.[33]

Both PS and PMMA favor the Au particle surface, while interfacial tension between the toluene molecules and the Au particle is relatively large. The effective polymer–Au attraction can lead the grafted polymers to shield the Au surface from toluene molecules, resulting in dense wetting layers of PS and PMMA blends in the vicinity of the nanoparticles. We hypothesize that the dense layer plays a decisive role in the formation of a phase-separated structure in the system. In addition, one may wonder whether demixing of ligands occurs during the synthesis step or after attaching the ligands on Au surface. Although the detailed mechanisms of Au particle formation still remain debatable, Li et al. proposed that after $NaBH_4$ reduction of Au ions, the thiol-terminated ligands diffuse into "naked" Au particles to form the Au–S bonds in an organic solvent (toluene) medium.[36] According to this scenario, the concentration of ligands is very dilute in toluene when ligands are attaching to the Au particles, and hence, the segregation power is significantly diminished. Since both PS and PMMA ligands are well dispersed and miscible in toluene, it is reasonable that the ligands are randomly attached to Au nanoparticles. Then, these ligands are phase separated on the

DOI: 10.1021/acsmacrolett.5b00101
ACS Macro Lett. 2015, 4, 417–421

Au nanoparticles due to the formation of dense wetting layer, as we have discussed.

To further examine the polymer morphology around the nanoparticle for the Mixed cases, we also simulated a model system using the dynamic Metropolis Monte Carlos method with a single site bond fluctuation model.[37−39] For the simulation, a particle coated with two types of end-grafted polymers in solvent is modeled by bead−spring-like A- and B-chains grafted to a stationary lattice cluster in the simulation box (the empty space being the solvent media). The lattice cluster as model particle is a very simplified model to mimic Au nanoparticle. However, this cluster artifact is qualitatively reflective of quasi-spherical shape of Au particle with many facets. For the chain dynamics of polymer ligands, the chain ends grafted to the surface are constrained to stay on the particle surface but allowed to migrate from one surface site to its neighboring sites to model the surface diffusion of the terminal thiol groups physisorbed on Au surface,[17,40] while the other unconstrained beads in the chain move according to Rouse-like bead relaxations. We assume the free slip motion of grafted chain ends on the particle surface, whereas in reality there is friction undergone by the motion of the terminal thiol groups on Au atomic surface. Also, the model does not include hydrodynamic interactions. These simplifications, however, affect dynamic properties but have little effects on the phase behavior of polymer ligands. The molecular characteristics in the model were set to approximate the Mixed ligand grafted on Au nanoparticles: the number of beads per grafted chain (N = 6, 14, 30), the particle radius ($R = 2a$ where a is the lattice spacing corresponding to approximately 1 nm), the grafting density ($\rho = 1.5a^{-2}$), and the pairwise interaction parameters between components. The interaction energy between unlike chain beads (ε_{AB}), the bead−particle interaction energy (ε_{AP}, ε_{BP}), and the solvent−particle interaction energy (ε_{SP}) are given as $\varepsilon_{AB} = \varepsilon_{AP} = \varepsilon_{AP} = \varepsilon_{SP}/3 = \varepsilon = 0.2\ k_BT$, and all other pairwise interaction energies (ε_{AA}, ε_{BB}, ε_{PP}, ε_{SS}, ε_{AS}, ε_{BS}) are set to be null.

Figure 4a shows the simulated surface morphologies of polymer-grafted particles with N = 6, 14, and 30, which roughly correspond to Mixed-1, Mixed-2, and Mixed-3 in the experiment, respectively (based on the number of monomers per Kuhn segment for PS and PMMA and the χ estimation).[33,41,42] The images in each of the panels in Figure 4a show a snapshot of a polymer-grafted particle (left side) and the density cloud for beads showing the region of $\Phi_A(\mathbf{r}) > 0.01$ and $\Phi_B(\mathbf{r}) > 0.01$ (right side), where $\Phi_\alpha(\mathbf{r})$ is the time-averaged bead density for bead type α at a position $\mathbf{r}$ from the particle center. The simulated morphologies clearly demonstrate that the two types of end-grafted polymers become phase-separated, forming a Janus-like surface morphology as N increases, which shows good agreement with the experimental results.

Figure 4b presents the radial bead distribution $\Phi(r)$ $(=\sum_{|\mathbf{r}|=r}[\Phi_A(\mathbf{r}) + \Phi_B(\mathbf{r})]/\sum_{|\mathbf{r}|=r}1)$ as a function of the distance r from the particle center. Three distinctive regimes are identified: regime I where solvent is expelled ($\partial\Phi/\partial r > 0$) by chain beads ($r/a$ = 2−3), regime II of rapidly decreasing Φ (r/a = 3−5), and regime III showing a long-tailed distribution (r/a > 5). In regime I, the polymer ligands tend to surround the particle to reduce the contact area between solvent molecules and the particle surface, leading to the expulsion of solvent molecules from the vicinity of the particle surface. We infer that the solvent depletion near the surface is attributed to the arrangement of chain beads in the course of wrapping the

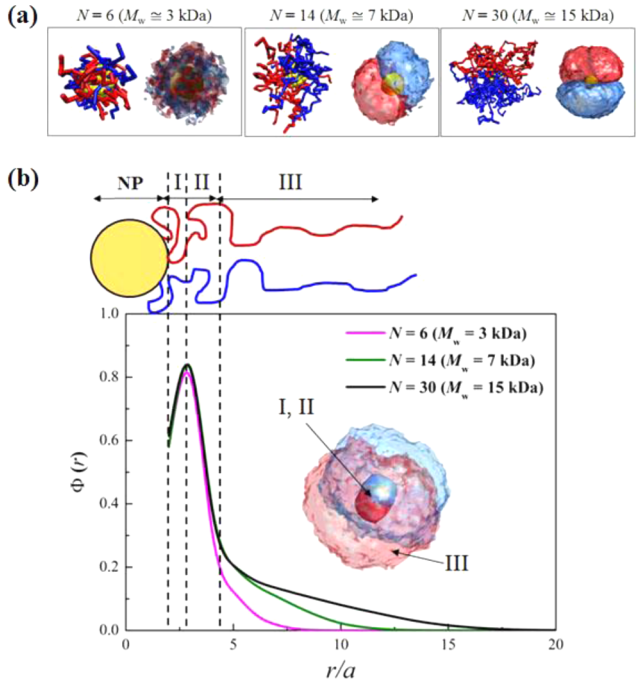

Figure 4. Monte Carlo simulation results for polymer-grafted particle with N = 6, 14, and 30 for $\varepsilon = 0.2\ k_BT$: (a) Simulated surface morphologies; (b) The radial bead distribution $\Phi(r)$. The images in each of the panels in (a) represent the snapshot of chain conformations (left side) and the density cloud of chain beads showing the region of $\Phi_A(\mathbf{r}) > 0.01$ and $\Phi_B(\mathbf{r}) > 0.01$ (right side). The inset in (b) represents the density cloud of beads for N = 30 showing regimes I, II ($\Phi_A(\mathbf{r}) > 0.2$ and $\Phi_B(\mathbf{r}) > 0.2$) and III ($\Phi_A(\mathbf{r}) > 0.01$ and $\Phi_B(\mathbf{r}) > 0.01$).

particle surface. In regime II, on the other hand, solvent molecules are mixed with the beads, as they are distant from the particle surface, followed by regime III, where the beads are more dilute due to the radial stretching of the polymers. The bead density cloud for N = 30, as shown in the inset of Figure 4b, indicates that the surface morphology is still Janus-like in regime III in spite of the very low polymer concentration. This solvent-diluted, yet Janus-like, morphology is driven by the segregated domain pattern in the dense polymer layer (regime I), which rationalizes the formation of a Janus-type shell even under good solvent conditions.

In summary, we have investigated the phase behavior of Mixed polymer ligands attached to a spherical nanoscale surface using small-angle neutron scattering (SANS). It was revealed that two polymer ligands of high molecular weight show phase separation to form a Janus-type shell on the nanoparticle surface, whereas those of low molecular weight form either a mixed or partly demixed shell. The SANS results along with the model simulation suggest that the effective attraction between polymer ligands and the particle surface is the main driving force for the formation of Janus-like polymer-grafted nanoparticles. In addition, time-dependent study on the nanoparticles would reveal the mechanism to phase separation in detail, which suggests a promising future direction for experiments. These results improve our understanding of the structure of polymer-grafted inorganic nanoparticles, which will aid in designing nanoparticles and composite systems.

DOI: 10.1021/acsmacrolett.5b00101
ACS Macro Lett. 2015, 4, 417−421

■ ASSOCIATED CONTENT

Supporting Information

Experimental methods and additional TEM data. This material is available free of charge via the Internet at http://pubs.acs.org.

■ AUTHOR INFORMATION

Corresponding Authors

*E-mail: junehuh@korea.ac.kr.
*E-mail: joona@korea.ac.kr.
*E-mail: shchoi@hongik.ac.kr..

Notes

The authors declare no competing financial interest.

■ ACKNOWLEDGMENTS

This work was supported by the National Research Foundation of Korea (NRF) Grant funded by the Korean Government (MSIP; No. NRF-2013M2B2A4041278) and by the KIST Institutional Program (Project No. 2E24841-14-037). S.K. and J.B. also acknowledge the support by the Human Resources Development Program of KETEP grant (No. 20134010200600) funded by the Korea government Ministry of Trade, Industry and Energy.

■ REFERENCES

(1) Bansal, A.; Yang, H.; Li, C.; Cho, K.; Benicewicz, B. C.; Kumar, S. K.; Schadler, L. S. *Nat. Mater.* **2005**, *4*, 693−698.
(2) Rittigstein, P.; Priestley, R. D.; Broadbelt, L. J.; Torkelson, J. M. *Nat. Mater.* **2007**, *6*, 278−282.
(3) Rittigstein, P.; Torkelson, J. M. *J. Polym. Sci., Part B: Polym. Phys.* **2006**, *44*, 2935−2943.
(4) Liu, J.; Tanaka, T.; Sivula, K.; Alivisatos, A. P.; Fréchet, J. M. J. *J. Am. Chem. Soc.* **2004**, *126*, 6550−6551.
(5) Bockstaller, M. R.; Mickiewicz, R. A.; Thomas, E. L. *Adv. Mater.* **2005**, *17*, 1331−1349.
(6) Kang, D. J.; Kwon, T.; Kim, M. P.; Cho, C.-H.; Jung, H.; Bang, J.; Kim, B. J. *ACS Nano* **2011**, *5*, 9017−9027.
(7) Kim, J.; Green, P. F. *Macromolecules* **2010**, *43*, 1524−1529.
(8) Chiu, J. J.; Kim, B. J.; Kramer, E. J.; Pine, D. J. *J. Am. Chem. Soc.* **2005**, *127*, 5036−5037.
(9) Kim, B. J.; Chiu, J. J.; Yi, G. R.; Pine, D. J.; Kramer, E. J. *Adv. Mater.* **2005**, *17*, 2618−2622.
(10) Kim, B. J.; Bang, J.; Hawker, C. J.; Kramer, E. J. *Macromolecules* **2006**, *39*, 4108−4114.
(11) Kang, H.; Detcheverry, F. A.; Mangham, A. N.; Stoykovich, M. P.; Daoulas, K. C.; Hamers, R. J.; Müller, M.; de Pablo, J. J.; Nealey, P. F. *Phys. Rev. Lett.* **2008**, *100*, 148303.
(12) Li, Q.; He, J.; Glogowski, E.; Li, X.; Wang, J.; Emrick, T.; Russell, T. P. *Adv. Mater.* **2008**, *20*, 1462−1466.
(13) Jang, S. G.; Kim, B. J.; Hawker, C. J.; Kramer, E. J. *Macromolecules* **2011**, *44*, 9366−9373.
(14) Borrell, M.; Leal, L. G. *Langmuir* **2007**, *23*, 12497−12502.
(15) Yoo, M.; Kim, S.; Lim, J.; Kramer, E. J.; Hawker, C. J.; Kim, B. J.; Bang, J. *Macromolecules* **2010**, *43*, 3570−3575.
(16) Kim, S.; Yoo, M.; Kang, N.; Moon, B.; Kim, B. J.; Choi, S.-H.; Kim, J. U.; Bang, J. *ACS. Appl. Mater. Interfaces* **2013**, *5*, 5659−5666.
(17) Kim, B. J.; Bang, J.; Hawker, C. J.; Chiu, J. J.; Pine, D. J.; Jang, S. G.; Yang, S.-M.; Kramer, E. J. *Langmuir* **2007**, *23*, 12693−12703.
(18) Yan, L.-T.; Popp, N.; Ghosh, S.-K.; Böker, A. *ACS Nano* **2010**, *4*, 913−920.
(19) Walther, A.; Muller, A. H. E. *Soft Matter* **2008**, *4*, 663−668.
(20) Zhou, T.; Dong, B.; Qi, H.; Mei, S.; Li, C. Y. *J. Polym. Sci., Part B: Polym. Phys.* **2014**, *52*, 1620−1640.
(21) Hore, M. J. A.; Ford, J.; Ohno, K.; Composto, R. J.; Hammouda, B. *Macromolecules* **2013**, *46*, 9341−9348.
(22) Zhang, J.; Jin, J.; Zhao, H. *Langmuir* **2009**, *25*, 6431−6437.
(23) Erhardt, R.; Zhang, M.; Böker, A.; Zettl, H.; Abetz, C.; Frederik, P.; Krausch, G.; Abetz, V.; Müller, A. H. E. *J. Am. Chem. Soc.* **2003**, *125*, 3260−3267.
(24) Berger, S.; Synytska, A.; Ionov, L.; Eichhorn, K.-J.; Stamm, M. *Macromolecules* **2008**, *41*, 9669−9676.
(25) Liu, X.; Yu, M.; Kim, H.; Mameli, M.; Stellacci, F. *Nat. Commun.* **2012**, *3*, 1182.
(26) Wang, B.; Li, B.; Zhao, B.; Li, C. Y. *J. Am. Chem. Soc.* **2008**, *130*, 11594−11595.
(27) Wang, B.; Li, B.; Dong, B.; Zhao, B.; Li, C. Y. *Macromolecules* **2010**, *43*, 9234−9238.
(28) Voets, I. K.; Fokkink, R.; de Keizer, A.; May, R. P.; de Waard, P.; Cohen Stuart, M. A. *Langmuir* **2008**, *24*, 12221−12227.
(29) Fütterer, T.; Vliegenthart, G. A.; Lang, P. R. *Macromolecules* **2004**, *37*, 8407−8413.
(30) Ohno, K.; Morinaga, T.; Takeno, S.; Tsujii, Y.; Fukuda, T. *Macromolecules* **2007**, *40*, 9143−9150.
(31) Dukes, D.; Li, Y.; Lewis, S.; Benicewicz, B.; Schadler, L.; Kumar, S. K. *Macromolecules* **2010**, *43*, 1564−1570.
(32) A rough estimation for the scaling of brush height h ($=R_{ptcl} - R_{core}$) with respect to the chain length N (in unit of monomer length) and the grafting density ρ gives that $h \sim (N\rho^{1/3})^{\nu}$ with $\nu = 0.54$ and $h \sim (N\rho^{1/2})^{\nu}$, with $\nu = 0.55$, respectively (Figure S1), which suggest that the polymer ligands is in the regime of in the regime of semidilute brush (SDB) rather than in the regime of concentrated brush (CB), based on the theoretical scaling form for spherically grafted polymers.[30,31] This was supported by the scaling analysis from the simulation results, which found $h \sim N^{0.59}$ (Figure S2).
(33) Owens, D. K.; Wendt, R. C. *J. Appl. Polym. Sci.* **1969**, *13*, 1741−1747.
(34) Russell, T. P.; Hjelm, R. P.; Seeger, P. A. *Macromolecules* **1990**, *23*, 890−893.
(35) Russell, T. P. *Macromolecules* **1993**, *26*, 5819−5819.
(36) Li, Y.; Zaluzhna, O.; Xu, B.; Gao, Y.; Modest, J. M.; Tong, Y. J. *J. Am. Chem. Soc.* **2011**, *133*, 2092−2095.
(37) Shaffer, J. S. *J. Chem. Phys.* **1994**, *101*, 4205−4213.
(38) Shaffer, J. S. *J. Chem. Phys.* **1995**, *103*, 761−772.
(39) Luettmer-Strathmann, J.; Mantina, M. *J. Chem. Phys.* **2006**, *124*, 174907.
(40) Wang, X.; Liu, Y.; Chen, Z.; Li, Y.; Sun, K.; Jiang, X. *J. Mater. Sci.* **2014**, *49*, 4394−4398.
(41) Fetters, L. J.; Lohse, D. J.; Richter, D.; Witten, T. A.; Zirkel, A. *Macromolecules* **1994**, *27*, 4639−4647.
(42) Jo, W. H.; Jang, S. S. *J. Chem. Phys.* **1999**, *111*, 1712−1720.

DOI: 10.1021/acsmacrolett.5b00101
ACS Macro Lett. 2015, 4, 417−421